^{127}I-NQR, ^{119}Sn Mössbauer Effect, and Electrical Conductivity of $MSnI_3$ (M = K, NH_4, Rb, Cs, and CH_3NH_3)*

Koji Yamada, Takashi Matsui, Tomoko Tsuritani, Tsutomu Okuda, and Sumio Ichiba

Department of Chemistry, Faculty of Science, Hiroshima University, Higashisenda-machi, Naka-ku, Hiroshima 730

Z. Naturforsch. **45a**, 307–312 (1990); received August 24, 1989; in revised form October 28, 1989

In a series of $MSnI_3$ compounds (M = K, NH_4, Rb, Cs, CH_3NH_3) two types of coordination around the central Sn(II) were found by ^{127}I-NQR and powder X-ray diffraction techniques. They are square pyramidal (for M = NH_4, Rb) and octahedral (for M = CH_3NH_3). $CsSnI_3$, on the other hand, showed a drastic structural change of the anion at 425 K from a square pyramid to a regular octahedron. Associated with this phase transition, the electrical conductivity increased from 4×10^{-3} S cm^{-1} to about 10^2 S cm^{-1}. This metallic modification was characterized by ^{127}I-NQR and ^{119}Sn Mössbauer spectroscopy.

Key words: NQR, Mössbauer effect, Perovskite compound, Phase transition, Electrical conductivity.

Introduction

The SnX_3^- (X = halogen) is essentially a trigonal pyramid such as isoelectronic SbX_3, having lone-pair electrons toward the three-fold axis. In the crystal lattice, however, not only the trigonal pyramid but also square pyramid or octahedral coordination due to halogen bridging appears [1–3]. In a cubic perovskite such as $CsSnBr_3$ [4, 5] and $CH_3NH_3SnBr_3$ Sn(II) is coordinated octahedrally by Br^- [2]. In these complexes the mainly available bonding-orbitals of Sn(II) are the 5p-orbitals because the 5s-orbital is occupied by a lone-pair and the 5d-energy levels are too high. This situation is called the hypervalent state of Sn(II). The linear X–Sn–X fraction is similar to the I_3^--anion having the three-center-four-electron bond (3c–4e) proposed by Pimentel [6, 7]. From the simple MO approach or halogen NQR-frequency, the 3c–4e bond has been recognized to have a higher ionic character than the normal 2c–2e bond. Furthermore, the 3c–4e bond distorts with decreasing temperature from, symmetric X–M–X to asymmetric X–M $\cdots$ X, in some cases, such as observed in $C_5H_5NHSbBr_4$ and $KSnBr_3 \cdot H_2O$ [1, 8]. At the asymmetric extreme, this bonding could be regarded as a normal 2c–2e bond. Indeed, two quite different structures for the I_3^--anion, symmetric and asymmetric, have been found [9, 10]. The structural variety of SnI_3^- stated above could be understood as a deformation of the 3c–4e bond in the three orthogonal directions.

The perovskites $CsSnI_3$ and $CH_3NH_3SnI_3$ have extremely high electrical conductivity. Most $MSnI_3$ compounds are yellow to orange, but the crystals having perovskite structure are black and have a metallic luster. These anomalous physical properties may be closely related to the linear –I–Sn–I–Sn– chain formed in the perovskite lattice. In this study the structures of the anion and the anomalously high electrical conductivity of the perovskites are discussed on the basis of ^{127}I-NQR and ^{119}Sn Mössbauer spectroscopy.

Experimental

SnI_2 was prepared by heating stoichiometric amounts of SnI_4 and Sn-metal in an evacuated tube at 350 °C for a week and was further purified by a Bridgman technique. All compounds except $CH_3NH_3SnI_3$ were crystallized from the melt. $CH_3NH_3SnI_3$ was prepared by a solid state reaction at 200 °C from well powdered CH_3NH_3I and SnI_2 in an evacuated tube.

The 4-probe method was employed to measure the electrical conductivity using a single crystal or a pressed powder sample. NQR spectra were observed

* Presented at the Xth International Symposium on Nuclear Quadrupole Resonance Spectroscopy, Takayama, Japan, August 22–26, 1989.

Reprint requests to Dr. Koji Yamada, Department of Chemistry, Faculty of Science, Hiroshima University, Naka-ku, Hiroshima 730, Japan.

0932-0784 / 90 / 0300-0307 $ 01.30/0. – Please order a reprint rather than making your own copy.

by means of a Matec pulsed spectrometer. The relaxation times T_1 were determined by a three pulse method, $180°-\tau-90°-180°$ echo. The recovery of the echo intensity could be expressed using a single time constant. ^{119}Sn Mössbauer spectra were recorded at 115 K by means of a constant acceleration type spectrometer using $Ca^{119m}SnO_3$ as a radiation source.

Results and Discussion

1. Powder X-Ray Diffraction, DTA, and Electrical Conductivity

According to the structural analysis reported by Mauersberger and Huber [11], SnI_3^- consists of distorted (SnI_6)-octahedra forming double chains along the *c*-axis (Figure 1 A). Thus there are three different bonding for the iodines, i.e. terminal, bridge, and triply bridge iodines (hereafter abbreviated as I(1), I(2) and I(3), respectively). The coordination around Sn(II) is regarded as a square pyramid having one short Sn–I bond (2.941 Å) and four Sn–I bonds on the basal plane (3.197–3.227 Å). The grown $CsSnI_3$ single crystal was black, but it turned to green after grinding. The powder X-ray pattern of this green sample was consistent with that simulated from the orthorhombic $CsSnI_3$ data reported in [11]. $RbSnI_3$ was isomorphous with $CsSnI_3$ (see Table 1); the indexing of the (*hkl*) reflections was unsuccessful, however, for NH_4SnI_3 and $KSnI_3$. As will be described later, the ^{127}I-NQR spectra for M = NH_4 and Rb resemble to that of $CsSnI_3$, suggesting similar $(SnI_3)_n^{n-}$-chains in these crystals. The black crystal of $CH_3NH_3SnI_3$ showed a cubic perovskite pattern with $a = 6.231$ Å, so that the Sn(II) site has an O_h symmetry with six 3.116 Å Sn–I bonds. DTA was observed for M = K, NH_4, Cs, and CH_3NH_3 in the temperature range 100–450 K. Below 295 K no heat anomaly was observed in the DTA curves for M = K, NH_4, and Cs, but with increasing temperature exothermic peaks were observed at 342 K, 416 K, and 425 K, respectively. The compounds, except M = Cs, returned to the low temperature phases. The high temperature phase of $CsSnI_3$, however, remained black and slowly returned to the green phases $CsSnI_3$(G) (hereafter the abbreviations (B) and (G) are used for the two phases). The black phase has a perovskite structure similar to $CH_3NH_3SnI_3$ and is stable if quenched to 77 K. Hence, ^{127}I-NQR, ^{119}Sn Mössbauer spectra and the electrical conductivity were measured for $CsSnI_3$(B)

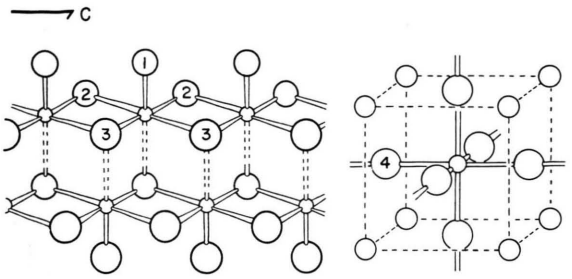

Fig. 1. Structure of SnI_3^--anions in (A) $CsSnI_3$ and (B) $CH_3NH_3SnI_3$. In these structures four different bonding types, i.e. I(1): terminal, I(2): bridge, I(3): triply-bridge, and I(4): linear-bridge.

Table 1. Crystallographic data for a series of $MSnI_3$ at room temperature.

Compound	Color	Crystal system	Lattice constant/Å
$RbSnI_3$	orange	ortho-rhombic	$a = 10.163$; $b = 17.291$; $c = 4.718$
$CsSnI_3$(G)	green	ortho-rhombic	$a = 10.328$; $b = 17.677$; $c = 4.765$ [a]
$CsSnI_3$(B)	black	tetragonal	$a = 6.13$; $c = 6.17$
$CH_3NH_3SnI_3$	black	cubic	$a = 6.231$

[a] Ref. [11].

in detail. Part of the NQR and DTA results for M = Cs and CH_3NH_3 have been reported previously [3].

Figure 2 shows the electrical conductivity of $CsSnI_3$ and $CH_3NH_3SnI_3$ as functions of temperature. The pellet sample prepared from $CsSnI_3$(G) showed a semiconductor type behavior below T_{tr} (425 K), but at T_{tr} an increase of the conductivity by four orders of magnitude was observed, associated with the phase transition from $CsSnI_3$(G) to $CsSnI_3$(B). On the other hand, a single crystal of $CsSnI_3$ obtained from the melt was essentially $CsSnI_3$(B), but the conductivity was not so high due to the formation of $CsSnI_3$(G) on the surface. Hence, the conductivity of $CsSnI_3$(B) was measured after heating the single crystal above T_{tr} (see Figure 2). The conductivity for $CsSnI_3$(B) increased gradually with decreasing temperature, such as observed for metals. This extremely high conductivity may be closely related to the perovskite lattice in which infinite linear –I–Sn–I–Sn– chains are formed three dimensionally.

2. ^{127}I-NQR Spectra and Relaxation

Because of the existence of three different bonding schemes, ^{127}I-NQR was observed over the wide frequency region from 20 to 140 MHz. As Table 2 shows, the ^{127}I-NQR spectra resembling to each other suggest that the M = NH_4, Rb, and Cs(G) analogues are isomorphous. In the case of $KSnI_3$, more than 8 lines were observed in the range 50–140 MHz, but neither the assignment nor the model structure could be deduced. Perovskite $CsSnI_3$(B), on the other hand, showed extremely broad $\nu_1(1/2 \leftrightarrow 3/2)$ transitions with an intensity ratio of 2:1, and the splitting between them decreased with increasing temperature as is shown in Figure 3. These findings, together with the reported powder X-ray diffraction, suggest that a tetragonal distortion takes place already at room temperature [3]. Heat anomalies were also observed in our previous DTA-curves for $CsSnI_3$(B) at 352 and 425 K, but it was not established which anomaly corresponds to the phase transition from tetragonal to cubic. A single ^{127}I-NQR ν_1-line was also expected at around 90 MHz for the cubic perovskite $CH_3NH_3SnI_3$, but not detected.

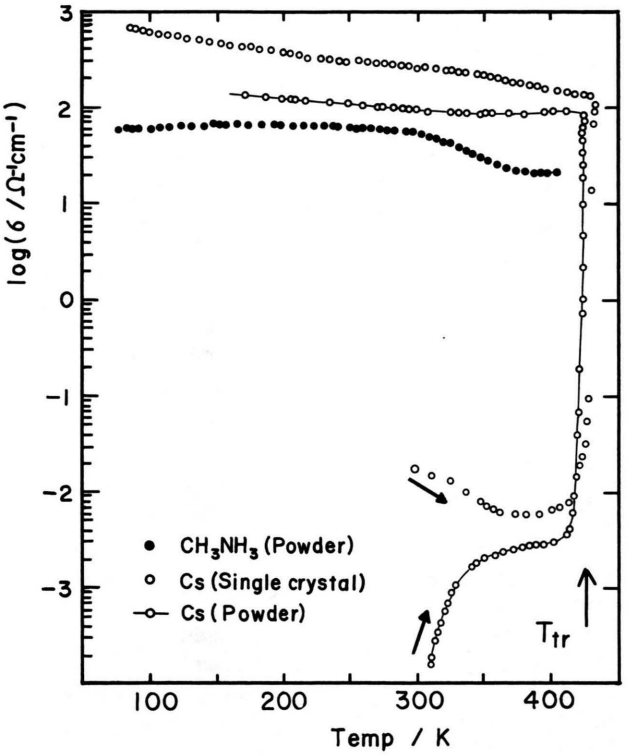

Fig. 2. Temperature dependence of the electrical conductivity of $CsSnI_3$ and $CH_3NH_3SnI_3$.

The asymmetry parameters shown in Table 2 are relatively large even for the terminal iodines, suggesting a large contribution from the lattice to the electric field gradient (efg) at the iodine site. In the first order approximation, however, the quadrupole coupling constant at the iodine is expressed as an imbalance of the iodine 5p-electrons, i.e.

$$(e^2Qq_{obs})/(e^2Qq_p) = |N_z - (N_y + N_x)/2|, \quad (1)$$

where N_z, N_y, and N_x are the populations of the $5p_z$, $5p_y$, and $5p_x$ orbitals, respectively, and $e^2Qq_p/h = 2293$ MHz. The Sn–I–Sn bond angles are close to 90° or 180° in all cases. Then (1) reduces to the following equations depending upon the bonding type in Fig. 4, assuming a lone-pair ($N = 2$) for the non-bonding directions:

$$\text{I(1) and I(4):} \quad (e^2Qq_{obs})/(e^2Qq_p) = |N_z - 2|,$$
$$\text{I(2):} \quad (e^2Qq_{obs})/(e^2Qq_p) = |N_x - 2|,$$
$$\text{I(3):} \quad (e^2Qq_{obs})/(e^2Qq_p) = |N_z - N_x|. \quad (2)$$

Table 2. ^{127}I-NQR parameters for $MSnI_3$ at 77 and 293 K [a].

Compound	ν_1/MHz	ν_2/MHz	e^2Qqh^{-1}/MHz	η	Assignment
NH_4SnI_3	20.42	36.89	125.0	0.290	I(3)
	52.88 (52.59)	99.35 (96.50)	334.5 (326.2)	0.225 (0.267)	I(2)
	72.59 (72.58)	122.03	418.6	0.394	I(1)
$RbSnI_3$	23.42	40.66	138.7	0.350	I(3)
	55.26 (54.58)	97.73 (95.74)	332.3 (326.0)	0.324 (0.326)	I(2)
	78.34 (76.58)	135.46 (134.69)	462.4 (458.5)	0.356 (0.332)	I(1)
$CsSnI_3$(G)	25.30	43.10	147.5	0.376	I(3)
	58.25 (56.86)	99.50 (97.42)	340.4 (333.1)	0.373 (0.369)	I(2)
	81.29 (79.59)	138.70 (137.64)	474.5 (4.69.8)	0.374 (0.356)	I(1)
$CsSnI_3$(B)	88.6 (88.2)		591 (588) [b]	0 (assumed)	I(4)
	94.2 (90.5)		628 (603) [b]	0 (assumed)	I(4)

[a] Values for 293 K in brackets.
[b] Calculated assuming $\eta = 0$.

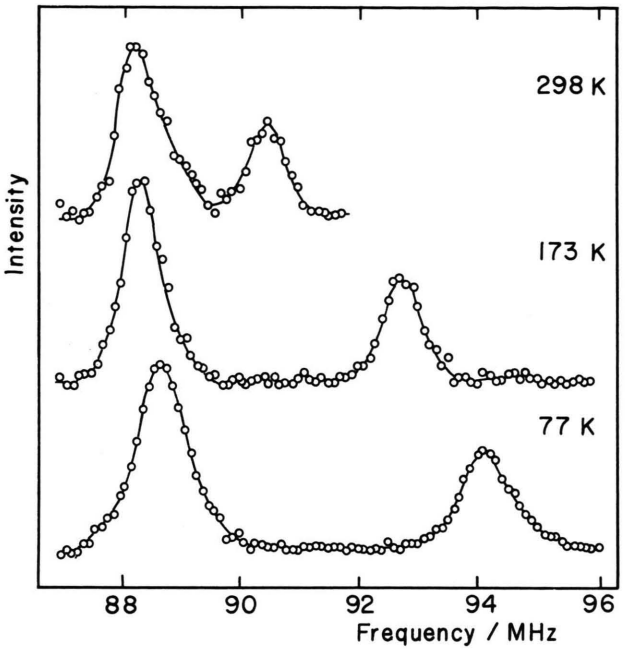

Fig. 3. ^{127}I-NQR spectra for $CsSnI_3$(B) at 77, 173, and 298 K by means of a spin echo method.

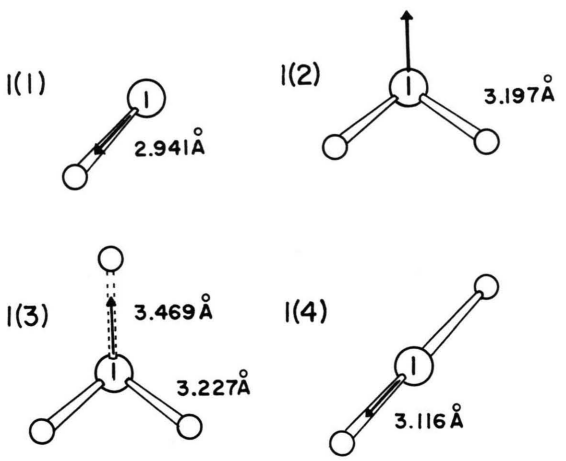

Fig. 4. Four different bonding schemes of iodines with expected q_{zz}-directions. I(1), I(2), and I(3) are iodines in orthorhombic $CsSnI_3$, and I(4) in perovskite $CH_3NH_3SnI_3$. I(2) an I(3) are located on a mirror perpendicular to the Sn–I–Sn plane.

In Table 3 the p-orbital populations and net charges, estimated from the NQR-parameters of $CsSnI_3$(G) and (B), are summarized.

Figure 5 shows the NQR spin-lattice relaxation times plotted against the temperature, where ν_1 transi-

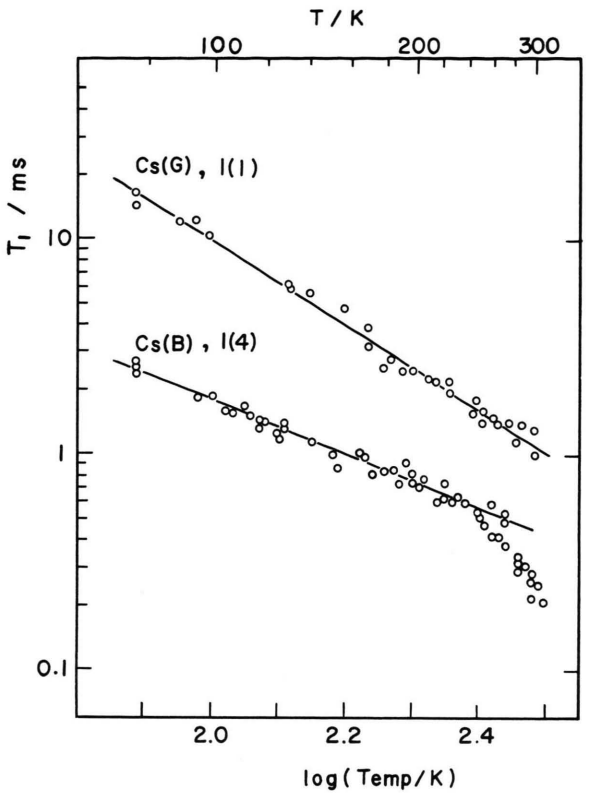

Fig. 5. Temperature dependence of the ^{127}I-NQR spin-lattice relaxation times T_1 for $CsSnI_3$(B) and $CsSnI_3$(G).

Table 3. p-Orbital populations and net charges for the four iodines having different bonding schemes.

Iodine	N_x	N_y	N_z	Net charge
I(1)	2	2	1.80	0.80
I(2)	1.86	1.86	2	0.71
I(3)	1.86 [a]	1.86	1.92	0.63
I(4)	2	2	1.75	0.75

[a] N_x is assumed 1.86 since the bond length is almost the same as that of the I(2) bridge.

tions assigned to I(1) and I(4) were used for the two modifications of $CsSnI_3$. As expected from the quite different electric properties for the two phases, different behaviors on temperature were observed. In the absence of the onset of reorientation of the anion, the NQR spin-lattice relaxation time (T_1) is expressed as

$$(1/T_1)_{obs} = (1/T_1)_{ele} + (1/T_1)_{vib} = a \cdot T + b \cdot T^2, \quad (3)$$

where the first and second terms represent the contributions from the conduction electrons and the lattice

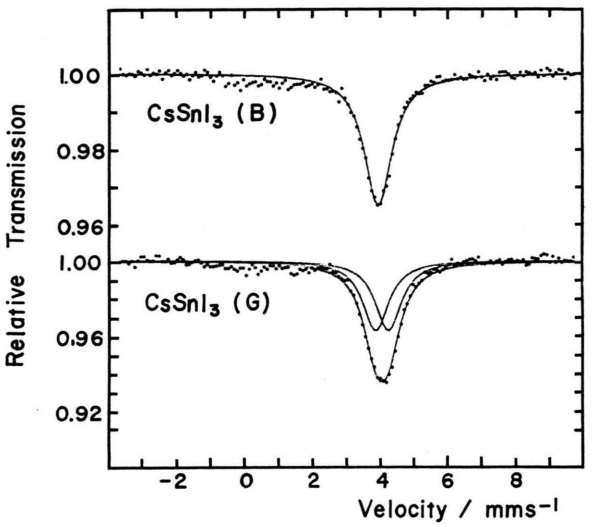

Fig. 6. ^{119}Sn Mössbauer spectra for the two modifications of $CsSnI_3$ at 115 K.

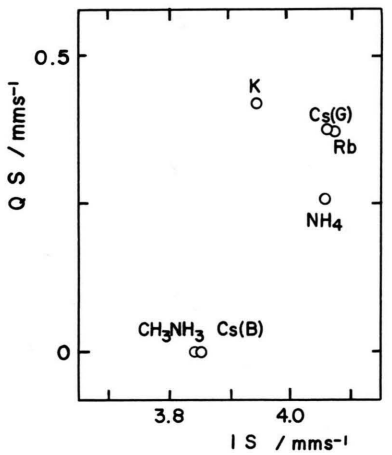

Fig. 7. Correlation between ^{119}Sn Mössbauer parameters, isomer shift (IS) and quadrupole splitting (QS).

vibrations, respectively. The slope of $\log(T_1)/\log(\text{Temp})$ in Fig. 5 is expected to be -2 if only the second term contributes to the relaxation similar to the system containing $I=3/2$ nuclei. Experimentally determined slopes are 1.91 ± 0.05 and 1.20 ± 0.5 for Cs(G) and Cs(B), respectively. These values suggest that the relaxation in Cs(B) is mainly governed by conduction electrons which seems to localize on the probe iodine. If the contribution from the second term, $(1/T_1)_{\text{vib}}$, is subtracted assuming parameters obtained for Cs(G), the slope reduces to 1.01, which agrees well with the theoretical expectation for electronic conductors. The deviation from this line above 250 K is probably due to the phase transition from tetragonal to cubic.

Table 4. ^{119}Sn Mössbauer parameters for $MSnI_3$ at 115 K.

Compound	Structure	IS mm/s	QS [a] mm/s
$KSnI_3$		3.94	0.42
NH_4SnI_3	square pyramid	4.06	0.26
$RbSnI_3$	square pyramid	4.02	0.37
$CsSnI_3$(G)	square pyramid	4.03	0.37
$CsSnI_3$(B)	octahedron	3.85	0
$CH_3NH_3SnI_3$	octahedron	3.84	0

[a] Quadrupole splittings were calculated assuming the linewidth parameter = 0.94 mm/s, which was deduced from perovskite $CH_3NH_3SnI_3$.

3. ^{119}*Sn Mössbauer Effect*

Figure 6 shows the ^{119}Sn Mössbauer spectra for $CsSnI_3$(G) and $CsSnI_3$(B), which were assigned to Sn(II) atoms with square pyramidal and regular octahedral coordination, respectively. The ^{119}Sn Mössbauer spectrum corresponding to the square pyramidal coordination was essentially a doublet, but the splitting is smaller than 1/2 of the respective linewidth. Consequently, each doublet was analyzed having the same linewidth as that of the perovskite $CH_3NH_3SnI_3$. Table 4 summarizes the ^{119}Sn Mössbauer parameters, quadrupole splitting (QS) and isomer shift (IS), at 115 K. In order to see the correlation between Mössbauer parameters and their structures, Fig. 7 plots QS against IS. From the standpoint of the spherical coordination in the perovskite lattice, a high IS value in the order of 4.05 mm s^{-1} is expected. The observed IS for the perovskite compounds, however, is much smaller than expected. According to Parish, IS depends directly on the valence-shell s-population and indirectly on the p-population by shielding, and is empirically expressed as [12]

$$\text{IS} = 2.7\,N_s - 0.15\,N_p\,, \tag{3}$$

where N_s and N_p are the population of the tin 5s- and 5p-orbitals. This unusually small IS is consistent with the band structure proposed by Clark et al. [13] for the interpretation of the semi-metalic $CsSnBr_3$, i.e. (3) suggests the donation of 0.07 s-electrons into a conduction band for $CsSnI_3$(B) and $CH_3NH_3SnI_3$.

[1] K. Yamada, T. Hayashi, T. Umehara, T. Okuda, and S. Ichiba, Bull. Chem. Soc. Japan **60,** 4203 (1987).
[2] K. Yamada, S. Nose, T. Umehara, T. Okuda, and S. Ichiba, Bull. Chem. Soc. Japan **61,** 4265 (1988).
[3] K. Yamada, T. Tsuritani, T. Okuda, and S. Ichiba, Chem. Lett. 1325 (1989).
[4] D. E. Scaife, P. F. Weller, and W. G. Fisher, J. Solid State Chem. **9,** 308 (1974).
[5] J. Barrett, S. R. A. Bird, J. D. Donaldson, and J. Silver, J. Chem. Soc. A **1971,** 3105.
[6] G. C. Pimentel, J. Chem. Phys. **19,** 446 (1951).
[7] T. A. Albright, J. K. Burdett, and M. H. Whangbo, Orbital Interaction in Chemistry, p. 258, John Wiley & Sons, New York 1985.
[8] T. Okuda, K. Yamada, H. Ishihara, M. Hiura, S. Gima, and H. Negita, J. Chem. Soc. Chem. Commun. **1981,** 979.
[9] R. C. L. Mooney Stater, Acta Crystallogr. **12,** 187 (1959).
[10] G. Migchelsen and A. J. T. Finney, Acta Crystallogr. Sect. B, **26,** 904 (1970).
[11] P. Mauersberger and F. Huber, Acta Crystallogr. Sect. B **36,** 683 (1980).
[12] R. V. Parish, Mössbauer Spectroscopy Application to Inorganic Chemistry (Gray J. Long, ed), Vol. 1, p. 527, Plenum Press, New York 1984.
[13] S. J. Clark, C. D. Flint, and J. D. Donaldson, J. Phys. Chem. Solid **42,** 133 (1981).